Synthesis, α-Glucosidase Inhibition, α-Amylase Inhibition and Molecular Docking Studies of 3,3-Di(Indolyl)Indolin-2-Ones

Mardi Santoso (tsv09@chem.its.ac.id)
Institut Teknologi Sepuluh Nopember https://orcid.org/0000-0003-0636-8386
Li Ong
Nanyang Technological University
Nur Aijijiyah
Institut Teknologi Sepuluh Nopember
First Wati
Institut Teknologi Sepuluh Nopember
Azminah Azminah
Universitas Surabaya
Rose Annur
Institut Teknologi Sepuluh Nopember
Arif Fadlan
Institut Teknologi Sepuluh Nopember
Kamilia Mustikasari
Institut Teknologi Sepuluh Nopember
Nila Huda
Institut Teknologi Sepuluh Nopember
Zaher Judeh
Nanyang Technological University

Research Article

Keywords: 3,3-Di(indoloyl)indolin-2-ones, Diabetes, α-Glucosidase inhibition, α-Amylase inhibition, Docking studies

Posted Date: May 6th, 2021

DOI: https://doi.org/10.21203/rs.3.rs-486324/v1

Version of Record: A version of this preprint was published at Heliyon on March 1st, 2022. See the published version at https://doi.org/10.1016/j.heliyon.2022.e09045.

Synthesis, α-glucosidase inhibition, α-amylase inhibition and molecular docking studies of 3,3-di(indolyl)indolin-2-ones

Mardi Santoso[1,✉] · Ong L. Lin[2,3] · Nur P. Aijijiyah[1] · First A. Wati[1] · Azminah Azminah[4] · Rose M. Annuur[1] · Arif Fadlan[1] · Kamilia Mustikasari[1] · Nila Huda[1] · Zaher M. A. Judeh[3]

[1] Department of Chemistry, Faculty of Science, Institut Teknologi Sepuluh Nopember, Sukolilo, Surabaya 60111, Indonesia

[2] NTU Institute for Health Technologies, Interdisciplinary Graduate School, Nanyang Technological University, Singapore, Research Techno Plaza, XFrontiers Block, #02-07, 50 Nanyang Drive, Singapore 637553

[3] School of Chemical and Biomedical Engineering, Nanyang Technological University, Singapore, 62 Nanyang Drive, N1.2–B1-14, Singapore 637459

[4] Department of Pharmaceutical Chemistry, Faculty of Pharmacy, University of Surabaya, Surabaya 60284, Indonesia

✉ Mardi Santoso

tsv09@chem.its.ac.id

Abstract

The synthesized 3,3-di(indoloyl)indolin-2-ones **1a**-**p** showed desired higher α-glucosidase inhibitory activities and lower α-amylase inhibitory activities than standard drug acarbose. Particularly, compound **1i** showed favourable higher α-glucosidase % inhibition of 67±13 and lower α-amylase % inhibition of 51±4 in comparison to acarbose with % inhibition activities of 19±5 and 90±2, respectively. Docking studies of selected 3,3-di(indoloyl)indolin-2-ones revealed key interactions with the active sites of both α-glucosidase and α-amylase, further supporting the observed % inhibitory activities. Furthermore, the binding energies are consistent with the % inhibition values. The results suggest that 3,3-di(indoloyl)indolin-2-ones may be developed as suitable Alpha Glucosidase Inhibitors (AGIs) and the lower α-amylase activities should be advantageous to reduce the side effects exhibited by commercial AGIS.

Keywords: 3,3-Di(indoloyl)indolin-2-ones · Diabetes · α-Glucosidase inhibition · α-Amylase inhibition · Docking studies

Introduction

Diabetes mellitus is a leading killer and fast-growing metabolic disease characterized by prolonged high levels of sugars in the blood (hyperglycemia) (Mitra et al., 2012). It occurs when the pancreas does not produce enough insulin (Type 1, ~ 10% of the cases) or when the body is not able to use the secreted insulin effectively (Type 2, ~ 90%) (Blair, 2016; DeFronzo et al., 2015). Prolonged hyperglycemia leads to complications including cardiovascular diseases, nephropathy, neuropathy, retinopathy etc (Blair, 2016; DeFronzo et al., 2015).

Current treatments of Type 2 diabetes focus on controlling hyperglycemia mainly through mediating glucose absorption and its removal from body tissues (Mitra et al., 2012; Blair, 2016).

One effective treatment choice is to use α-glucosidase inhibitors (AGIs) (Derosa and Maffioli, 2012). AGIs inhibit α-glucosidase enzyme, and hence control the level of glucose that enters the bloodstream. However, current AGIs also cause undesired strong inhibition of α-amylase enzymes. Upon eating, α-amylase enzymes in the saliva and pancreatic juices hydrolyzes α-1,4-glycosidic bonds (but not α-1,6 bonds) of starch to produce dextrins, disaccharides, and oligosaccharides (Afifi et al., 2008; Kwon et al., 2007). Consequently, α-glucosidase enzymes located at the brush border cells of the epithelium of the small intestine cleave the terminal, non-reducing 1,4-glycosidic bonds in disaccharides and oligosaccharides to produce α-D-glucose which then enters the bloodstream (Kim et al., 2005). Therefore, inhibition of α-glucosidase to control absorption of α-D-glucose is a favourable option to treat diabetics (Yoshikawa et al., 1998). Though commercial AGI drugs (Acarbose, Miglitol, and Voglibose) are very effective inhibitors of α-glucosidase, they also cause gastrointestinal side-effects such as flatulence, diarrhoea, bloating, abdominal pain and discomfort (Derosa and Maffioli, 2012). These side-effects are attributed to strong inhibition of α-amylase since undigested carbohydrates accumulate in the colon and get fermented by gut bacteria causing these side-effects (Kelley et al., 1998). Therefore, it is desirable to design new selective AGIs having strong inhibition of α-glucosidase and low inhibition of α-amylase.

Indole-based compounds are abundant in the plant kingdom and show many bioactivities including antimalarial (Santos et al., 2015), antifungal (Song et al., 2015), anticancer (El Sayed et al., 2015), antibacterial (Gali et al., 2015), antihelmintic (Srivastava et al., 1999), and anti-diabetic (Gali et al., 2015) activities (Chadha and Silakari, 2017). Several indole-based drugs such as Sunitinib, indolidan, delaverdine, indomethacin, indoxole and vinblastine are marketed for the treatment of various diseases while others are at various stages of clinical trials (Chadha and Silakari, 2017; Zhang et al., 2015; Khan et al., 2014).

Oxindoles also exhibit many activities including antiviral, antimicrobial, antifungal, anticancer, anti-inflammatory, antihypertensive, serotonergic, analgesic and sleep-inducing activities (Khan et al., 2014). Oxindoles of the 3,3-di(indolyl)indolin-2-ones type (Scheme 1) show antidiabetic (Wang et al., 2017), anticancer (Karimi et al., 2015), antimicrobial (Reddy et al., 2012) and spermicidal (Paira et al., 2009) activities. Recently, Wang and co-workers (Wang et al., 2017) reported promising α-glucosidase inhibition activities of several 3,3-di(indolyl)indolin-2-ones. However, the authors did not examine the α-amylase inhibition activities which are important for developing next-generation AGIs having minimal gastrointestinal side-effects. They also did not elucidate the structure activity relationship of 3,3-di(indolyl)indolin-2-ones with aromatic substituents as well as strongly donating and withdrawing moieties on inhibition of α-glucosidase. Therefore, at this stage, the overall inhibitory activity profile of 3,3-di(indolyl)indolin-2-ones remains unclear.

Herein, we report the synthesis of diverse 3,3-di(indolyl)indolin-2-ones and examine their α-glucosidase and α-amylase activities to provide a clear understanding of their overall inhibition effectiveness. To complement our study, we also report the molecular docking studies to elucidate the mechanism of action of these compounds.

Materials and Method

Materials

All starting materials and reagents were purchased from Sigma-Aldrich, Merck and Fluka, and were used without further purification. Thin layer chromatography was performed on Merck 0.20 mm precoated silica gel aluminum plates (Kieselgel 60, F_{254}) and visualized using UV lamp operating at 245 nm. Melting points were measured using Fischer-John apparatus and are

uncorrected. Infrared spectra were recorded from KBr disc using FTIR Shimadzu 8400S. NMR spectra were recorded using Jeol JNM-ECA300 (300 MHz), Jeol JNM-ECS400 (400 MHz), Bruker Avance DPX 300 (300 MHz) or Hitachi R-1900 FT NMR (90 MHz). Mass spectra were obtained using a Xevo G2-XS QTof, Hitachi QP-5000 or Waters LCT Premier XE instrument.

Chemistry

General Procedure for the Synthesis of 3,3-Di(indolyl)indolin-2-one

A solution of the isatin or its alkyl derivative and indole or its alkyl derivative in methanol (~100 ml per 1g of isatin) was treated with a catalytic amount of BF_3 or H_2SO_4 (2-3 drops per 1 g of isatin) and stirred at 40-60 ^oC for 1-2 h. After completion of the reaction as indicated by TLC, the reaction mixture was diluted with ice-cold water (50 mL per 1g of isatin). The resulting precipitates were filtered under vacuum, washed with excess of ice-cold water (3 x 50 mL) and then were dried under vacuum to give the pure product. This general procedure was used to prepare 3,3-di(indolyl)indolin-2-one derivatives (**1a**-**1c**, **1f**, **1i**-**1p**).

3,3-Di(1*H*-indole-3-yl)indolin-2-one (1a) Isatin (0.30 g, 2.04 mmol) and indole (0.47 g, 4.00 mmol) reacted to give **1a** as white powder (0.71 g, 97% yield), m.p. 320-321°C (lit (Suresh et al., 2016). 317-319 ^oC). ^1H NMR (90 MHz, DMSO-d_6): δ 6.70-7.40 (m, 14H), 10.54 (s, 2H), 10.91 (s, 1H). Mass spectrum (EI): *m/z* 363 (M, 80%), 334 (100), 247 (10), 219 (50).

3,3-Di(1-methyl-1*H*-indole-3-yl)indolin-2-one (1b) Isatin (0.25 g, 1.70 mmol) and 1-methylindole (0.44 g, 3.35 mmol) reacted to give **1b** as white powder (0.58 g, 88% yield), m.p. 329-330 °C (lit (Rad-Moghadam et al., 2010). mp >300 ^oC). ^1H NMR (90 MHz, $(CD_3)_2CO$): δ 3.76 (s, 6H), 6.74-7.45 (m, 14H), 9.45 (bs, 1H). Mass spectrum (EI): *m/z* 392 (M+1, 10%), 391 (M, 60), 376 (5), 362 (100), 233 (20).

3,3-Di(1-ethyl-1*H*-indole-3-yl)indolin-2-one (1c) A solution of isatin (0.052 g, 0.35 mmol) and 1-ethylindole (0.10 g, 0.69 mmol) reacted to give **1c** as white powder (0.13 g, 93% yield), m.p. 340-341°C (lit (Rad-Moghadam et al., 2010). mp >300 °C). ^{1}H NMR (90 MHz, $(CD_3)_2CO$): δ 1.28 (t, *J*=7.2 Hz, 6H), 4.14 (q, *J*=7.2 Hz, 4H), 6.73-7.47 (m, 14H), 10.56 (s, 1H). Mass spectrum (EI): *m/z* 420 (M+1, 10%), 419 (M, 65), 390 (100), 275 (15), 247 (10).

3,3-Di(1*H*-indole-3-yl)-5-bromoindolin-2-one (1f) 5-Bromoisatin (0.050 g, 0.22 mmol) and indole (0.050 g, 0.45 mmol) reacted to give **1f** as brown solid (0.090 g, 92% yield), m.p. 282-283 °C (lit (Karimi et al., 2015). 299-301 °C). ^{1}H NMR (90 MHz, $(CD_3)_2CO$): δ 6.73-7.42 (m, 13H), 10.71 (s, 1H), 10.98 (s, 1H). Mass spectrum (EI): *m/z* 443 (M, ^{81}Br, 10%), 441 (M, ^{79}Br, 10), 327 (5), 325 (5), 299 (5), 297 (5), 44 (100).

3,3-Di(5-hydroxy-1*H*-indole-3-yl)-5-nitroindolin-2-one (1i) 5-Nitroisatin (0.096 g, 0.50 mmol) and 5-hydroxyindole (0.13 g, 1.00 mmol) reacted, and after column chromatography (ethyl acetate:*n*-hexane, 2:1), gave **1i** as brown solid (0.15 g, 68 % yield), m.p. 302-303 °C. IR (KBr disk): 3524, 3349, 3117, 1697, 1626, 1605, 1582, 1528, 1468, 1338, 1202, 1062 cm^{-1}. ^{1}H NMR (400 MHz, DMSO-d_6): δ 6.53 (dd, *J*= 8.4, *J* = 2.4 Hz, 4H), 6.57 (d, *J* = 2.4 Hz, 2H), 6.78 (d, *J*=2.4 Hz, 2H), 7.12-7.16 (m, 3H), 7.90 (d, *J* = 2.0 Hz, 1H), 8.20 (dd, *J*= 8.4, *J*=2.4 Hz, 1H), 8.52 (s, 2H), 10.72 (s, 1H), 10.73 (s, 1H), 11.20 (bs, 1H). ^{13}C NMR (100 MHz, DMSO-d_6): δ 53.1, 105.1, 110.3, 112.2, 112.6, 120.5, 125.6, 125.7, 125.9, 126.7, 132.1, 136.0, 142.7, 148.4, 150.5, 179.5.

3,3-Di(1*H*-indole-3-yl)-5-nitroindolin-2-one (1j) 5-Nitroisatin (0.072 g, 0.38 mmol) and indole (0.088 g, 0.75 mmol) reacted to give the **1j** as yellow solid (0.13 g, 87% yield), m.p. 272-273 °C (lit (Suresh et al., 2016). 277-279 °C). IR (KBr disc): 3385, 3123, 3059, 1709, 1620, 1528, 1481, 1456, 1420, 1340, 1246, 1215, 1175, 1129, 1086, 1013, 941 cm^{-1}. ^{1}H NMR (300 MHz, $(CD_3)_2CO$): δ 6.87 (t, *J*=4.6 Hz, 2H), 7.05-7.09 (m, 4H), 7.07 (s, 1H), 7.32 (d, *J*=9.1 Hz, 1H), 7.42 (d, *J*=5.1

Hz, 4H), 7.44 (d, *J*=4.8 Hz, 2H), 8,15 (d, *J*=1.5 Hz, 1H), 8.27 (dd, *J*=4.0, 1.5 Hz, 1H), 10.20 (bs, 1H), 10.29 (s, 2H). ^{13}C NMR (75 MHz, $(CD_3)_2CO$): δ 53.9, 110.6, 112.6, 114.7, 119.8, 121.6, 121.9, 122.5, 125.6, 126.1, 126.9, 136.6, 138.5, 143.9, 148.6, 179.5. MS (ES): *m/*z calcd for $C_{24}H_{15}N_4O_3$, $[M-H]^-$ 407.1144; Found 407.1124.

3,3-Di(1-methyl-1*H*-indole-3-yl)-5-nitroindolin-2-one (1k) 5-Nitroisatin (0.29 g, 1.51 mmol) and 1-methylindole (0.39 g, 2.97 mmol) reacted to give **1k** as yellow solid (0.61 g, 94% yield), m.p. 291-292 °C (lit (Rad-Moghadam et al., 2010). >300 ºC). ^{1}H NMR (300 MHz, $(CD_3)_2CO$): δ 3.78 (s, 6H), 6.88 (t, *J*=4.1 Hz, 2H), 7.00 (s, 2H), 7.12 (t, *J*=4.6 Hz, 2H), 7.31 (d, *J*=5.2 Hz, 1H), 7.37 (d, *J*=4.8 Hz, 2H), 7.41 (d, *J*=4.8 Hz, 2H), 8.12 (d, *J*=1.5 Hz,1H), 8.26 (dd, *J*=4.5, 1.4Hz, 1H), 10.29 (bs, 2H). ^{13}C NMR (125 MHz, $(CD_3)_2CO$): δ 32.9, 53.7, 110.6, 110.6, 113.6, 119.7, 121.6, 122.1, 122.5, 126.1, 127.3, 129.8, 136.6, 138.9, 143.9, 148.6, 179.4. MS (ES): *m/*z calcd for $C_{26}H_{19}N_4O_3$, $[M-H]^-$ 435.1457; Found 435.1436.

3,3-Di(1*H*-indole-3-yl)-1-benzyl-5-nitroindolin-2-one (1l) 1-Benzyl-5-nitroisatin (0.070 g, 0.25 mmol) and indole (0.060 g, 0.51 mmol) reacted to give **1l** as a yellow solid (0.10 g, 83% yield), m.p. 237-238 °C. IR (KBr disc): 3458, 3352, 3125, 3061, 1711, 1603, 1518, 1487, 1454, 1335, 1211, 1173, 1105, 1080, 748 cm^{-1}. ^{1}H NMR (400 MHz, DMSO-*d*$_6$): δ 5.09 (s, 2H), 6.74 (t, *J*=7.6 Hz, 2H), 6.95 (d, *J*=2.4 Hz, 2H), 7.01 (d, *J*=7.6 Hz, 2H), 7.07 (d, *J* = 8.6 Hz, 2H), 7.28-7.37 (m, 8H), 8.00 (d, *J*=2.4 Hz, 1H), 8.24 (dd, *J*=8.6, 2.4 Hz, 1H), 11.09 (s, 2H). ^{13}C NMR (400 MHz, DMSO-*d*$_6$): δ 43.9, 52.7, 110.2, 112.4, 113.0, 119.1, 120.4, 120.9, 121.8, 125.2, 125.8, 125.9, 128.2, 128.3, 129.3, 135.0, 136.3, 137.6, 143.4, 148.2, 177.9. HRMS (ES): *m/*z calcd for $C_{31}H_{21}N_4O_3$, $[M-H]^-$ 497.1614; Found 497.1636.

3,3-Di(1*H*-indole-3-yl)-1-benzyl-5-bromoindolin-2-one (1m) 1-Benzyl-5-bromoisatin (0.030 g, 0.10 mmol) and indole (0.020 g, 0.20 mmol) reacted to give **1m** as yellow solid (0.043 g, 81%

yield), m.p. 188-189 °C (lit (Karimi et al., 2015). 268-270 ºC). IR (KBr disc): 3428, 3356, 3131, 3063, 1699, 1603, 1546, 1479, 1454, 1422, 1341, 1242, 1213, 1173, 1101, 1065, 1013, 749 cm^{-1}. ^{1}H NMR (400 MHz, DMSO-d_6): δ 5.00 (s, 2H), 6.74 (t, *J*=8.0 Hz, 2H), 6.89 (d, *J*=2.8 Hz, 2H), 7.01 (t, *J*=7.6 Hz, 2H), 7.08 (t, *J*=7.0 Hz, 3H), 7.26-7.45 (m, 10H), 11.03 (s, 2H). ^{13}C NMR (400 MHz, DMSO-d_6): δ 43.6, 53.0, 112.0, 112.3, 113.7, 114.7, 119.0, 121.0, 121.7, 125.0, 125.9, 127.8, 128.1, 129.2, 131.3, 136.7, 136.7, 137.5, 141.6, 177.1. MS (ES): *m/*z calcd for $C_{31}H_{31}N_3OBr$, $[M-H]^-$ 530.0868; Found 530.0910.

3,3-Di(1*H*-indole-3-yl)-1-(4-bromobenzyl)-5-bromoindolin-2-one (1n) 1-(4-Bromo-benzyl)-5-bromoisatin (0.19 g, 0.48 mmol) and indole (0.12 g, 1.02 mmol) reacted to give **1n** as ivory coloured solid (0.28 g, 97% yield), m.p. 248-249 °C. IR (KBr disc): 3416, 3287, 3056, 1715, 1601, 1537, 1422, 1333, 1244, 1206, 1167, 1101, 1071, 1013, 741 cm^{-1}. ^{1}H NMR (400 MHz, DMSO-d_6): δ 4.97 (s, 2H), 6.73 (t, *J* =7.4 Hz, 2H), 6.87 (s, 2H), 7.00 (dd, *J*=12.8, 8.0 Hz, 4H), 7.13 (d, *J*=8.0 Hz, 1H), 7.28 (d, *J*=8.0 Hz, 2H), 7.35 (d, *J*=7.4 Hz, 3H), 7.45 (d, *J*=8.4 Hz, 1H), 7.49 (d, *J*=8.0 Hz, 2H), 11.02 (s, 2H). ^{13}C NMR (400 MHz, DMSO-d_6): δ 42.5, 52.4, 111.5, 111.9, 113.1, 114.3, 118.5, 120.5, 120.8, 121.2, 124.6, 125.4, 127.3, 130.0, 130.8, 131.6, 135.7, 136.1, 137.0, 140.9, 176.6. MS (ES): *m/*z calcd for $C_{31}H_{21}N_3OBr_2$, $[M+Na]^+$ 633.9929; Found 633.9542.

3,3-Di(1*H*-indole-3-yl)-5-chloroindolin-2-one (1o) 5-Chloroisatin (0.051 g, 0.28 mmol) and indole (0.065 g, 0.56 mmol) reacted to give **1o** as brown solid (0.10 g, 98% yield), m.p. 275-276 °C (lit (Suresh et al., 2016). 290-291 ºC). ^{1}H NMR (90 MHz, $CDCl_3$): δ 6.81-7.42 (m, 13H), 10.70 (s, 1H), 10.98 (s, 2H). Mass spectrum (EI): *m/z* 399 (M, ^{37}Cl, 10%), 397 (M, ^{35}Cl, 30), 368 (15), 246 (50), 117 (35), 44 (100).

3,3'-Di(1-methyl-1*H*-indole-3-yl)-5-chloroindolin-2-one (1p) 5-Chloroisatin (0.083 g, 0.46 mmol) and 1-methylindole (0.12 g, 0.92 mmol) reacted to give **1p** as pink solid (0.17 g, 89% yield),

m.p. 278-279 °C (lit (Brahmachari and Banerjee, 2014). >300 ºC). IR (KBr disc): 3223, 2932, 1717, 1616, 1541, 1476, 1429, 1371, 1333, 1290, 1248, 1200, 739 cm^{-1}. ^{1}H NMR (90 MHz, DMSO-d_6): δ 3.72 (s, 6H), 6.77-7.44 (m, 3H), 10.74 (s, 1H). ^{13}C NMR (23 MHz, DMSO-d_6): δ 32.3, 52.6, 109.7, 111.4, 112.5, 118.4, 120.5, 121.0, 124.5, 125.4, 125.7, 127.7, 128.4, 136.3, 137.2, 140.0, 177.9. Mass spectrum (EI): *m/z* 427 (M, ^{37}Cl, 5), 425 (M, ^{35}Cl, 15), 399 (30), 397 (10), 269 (9), 267 (3), 44 (100).

General Procedures for the Synthesis of Substituted 3,3-Di(indolyl)indolin-2-one through *N*-Alkylation

A mixture of the 3,3-di(indolyl)indolin-2-one and freshly crushed KOH in anhydrous DMSO was stirred at room temperature for 1 h. After cooling to ice-bath temperature, the alkylating agent was added and the mixture was stirred further at room temperature for 1 h. After completion of the reaction as indicated by TLC, the reaction mixture was diluted with ice-cold water (~50 mL per 0.5 mmol of starting indolin-2-one). The resulting precipitate was filtered under vacuum, washed with excess of ice-cold water (3 x 50 mL), and dried to give the pure product. This general procedure was used to make compounds **1d**, **1e**, and **1g**.

3,3-Di(1-methyl-1*H*-indole-3-yl)-1-methylindolin-2-one (1d) A mixture of **1b** (0.20 g, 0.51 mmol) and KOH (0.11 g, 1.96 mmol) in DMSO (15 mL) reacted with methyl iodide (0.06 mL, 0.96 mmol) to give **1d** as white solid (0.19 g, 90% yield), m.p. 218-219 °C (lit (Bergman and Eklund, 1980). 232-234 ºC). ^{1}H NMR ($CDCl_3$): δ 3.32 (s, 3H), 3.66 (s, 6H); 6.82-7.48 (m, 14H). Mass spectrum (EI): *m/z* 406 (M+1, 30%), 405 (M, 100), 390 (10), 376 (90), 275 (40), 247 (70), 233 (20).

3,3-Di(1-ethyl-1*H*-indole-3-yl)-1-ethylindolin-2-one (1e) A mixture of **1c** (0.10 g, 0.24 mmol) and KOH (0.066 g, 1.18 mmol) in anhydrous DMSO (10 mL) reacted with ethyl iodide (0.04 mL,

0.48 mmol) to give **1e** as white solid (0.10 g, 91% yield), m.p. 169-170 °C (lit (Kothandapani et al., 2018). 272-274 ºC). ^{1}H NMR ($CDCl_3$): δ 1.23-1.29 (m, 9H), 3.83 (q, *J*=6.0 Hz, 2H), 4.13 (q, *J*=6.0 Hz, 4H), 6.83 (t, *J*=9,0 Hz, 2H), 6.92 (s, 2H), 6.98-7.10 (m, 3H), 7.17-7.27 (m, 3H), 7.32 (d, *J*=6.0 Hz, 2Hz), 7.43 (d, *J*=9.0 Hz, 2H). Mass spectrum (EI): *m/z* 448 (M+1, 30%), 447 (M, 100), 418 (75), 404 (30), 390 (20), 303 (40), 275 (40), 247 (70), 233 (20).

3,3-Di(5-bromo-1-methyl-1*H*-indole-3-yl)-5-bromo-1-methylindolin-2-one (1g) A mixture of 3,3-di(5-bromo-1-methyl-*1H*-indole-3-yl)-5-bromoindolin-2-one (0.030 g, 0.048 mmol) and KOH (0.036 g, 0.64 mmol) in DMSO (15 mL) reacted with dimethyl sulfate (0.06 mL, 0.63 mmol) to give **1g** as light orange solid (0.029 g, 94% yield), m.p. 287-288 °C. IR (KBr disc): 2918, 1713, 1607, 1537, 1474, 1422, 1368, 1337, 1273, 1219, 1144, 1094, 1049, 789 cm^{-1}. ^{1}H NMR (500 MHz, $CDCl_3$): δ 3.25 (s, 3H), 3.73 (s, 6H), 7.02 (s, 2H), 7.21 (d, *J*=8.4 Hz, 1H), 7.23 (d, *J*=2.0 Hz, 1H), 7.25 (d, *J*=2.0 Hz, 1H), 7.27 (d, *J*=2.0 Hz, 1H), 7.31 (d, *J*=2.0 Hz, 1H), 7.43 (d, *J*=9.1 Hz, 2H), 7.59 (dd, *J*=8.4, 2.0 Hz, 1H). ^{13}C NMR (125 MHz, $CDCl_3$): δ 26.5, 32.7, 51.7, 111.2, 111.6, 111.7, 112.4, 114.4, 122.5, 123.9, 127.2, 130.2, 131.2, 134.8, 136.2, 141.8, 175.9. Mass spectrum (ES): *m/z* calcd for $C_{27}H_{21}Br_3N_3O$, $[M+H]^+$ 639.9235; Found 639.9280.

Reduction of 1j to 1h

3,3'-Di(1*H*-indole-3-yl)-5-5-aminoindolin-2-one (1h) A mixture of **1j** (0.10 g, 0.25 mmol) and Pd/C (0.01 g) in ethanol (10 mL) was brought to reflux. To this mixture, a solution of hydrazine hydrate (0.49 mL, 0.01 mmol) in ethanol (10 mL) was added dropwise. The resulting mixture was heated to reflux for 90 min, allowed to cool and then diluted with THF (5 mL). The cooled mixture was filtered and the mother liquor was diluted with water (50 mL). The resulting precipitates were filtered under vacuum, washed with excess of ice-cold water (3 x 50 mL), dried over $MgSO_4$, purified by column chromatography (chloroform:ethyl acetate, 1:2) to give **1h** as brown-yellow

solid (0.068 g, 72% yield), m.p. 258-259 °C. IR (KBr disc): 3626, 3364, 3315, 3121, 3057, 1666, 1614, 1491, 1456, 1421, 1335, 1244, 1207, 1103, 1014 cm^{-1}. ^{1}H NMR (400 MHz, DMSO-d_6): δ 5.11 (bs 2H), 6.44 (dd, *J*=8.0, 2.0 Hz, 1H), 6.52 (s, 1H), 6.66 (d, *J*=8.8 Hz, 1H), 6.75 (t, *J*=7.6 Hz, 2H), 6.79 (d, *J*=2.4 Hz, 2H), 6.97 (t, *J*=7.2 Hz, 2H), 7.20 (d, *J*=8.0 Hz, 2H), 7.30 (d, *J*=7.6 Hz, 2H), 10.15 (s, 1H), 10.88 (s, 2H). ^{13}C NMR (100 MHz, DMSO-d_6): δ 53.4, 110.3, 112.0, 113.1, 114.0, 115.3, 118.6, 121.4, 121.5, 124.8, 126.3, 132.3, 136.0, 137.4, 142.8, 179.0. Mass spectrum (ES): *m/z* calcd for $C_{24}H_{20}N_4O$, $[M+2H]^{2+}$ 380.1637; Found 380.4356.

α-Glucosidase Inhibition Assay

The procedure used for testing of α-glucosidase inhibitory activity was a modified version of that employed by Kang and co-workers (Kang et al., 2011). 8 µL of the tested compounds in DMSO corresponding to 50 µg/mL final concentration of the compounds in the net tested solution was added to 115 µL of 0.1 M sodium phosphate buffer pH 7.0 in a 96 well microtiter plate. To this mixture, 50 µL of α-glucosidase enzyme solution (0.5 U/mL of yeast α-glucosidase in buffer solution) was added. 'Blank' and 'Positive Control' were also prepared. For both, no inhibitor was added. Instead, 8 µL of DMSO wad added to equalize the volume. For 'Blank', 50 µL of buffer was added instead of the enzyme. Acarbose was used as the standard in this procedure. The microtiter plate was shaken at 37 ºC for 15 minutes. Next, 25 µL of 2.5 mM of 4-nitrophenyl β-D-glucopyranoside (PNPG) substrate (solution in the buffer) was added to each well. The entire plate was shaken at 37 ºC for another 15 minutes before measuring absorbance at 405 nm using a microplate reader. The percentage of inhibition is calculated using the following formula:

$$\left(\frac{\left(Abs_{positive\ control} - Abs_{compound}\right)}{Abs_{positive\ control}}\right) \times 100\ \%$$

All measurements are performed in triplicates and the values are represented as mean ± standard deviation.

α-Amylase Inhibition Assay

The procedure for testing α-amylase inhibitory activity was a modified version of the protocol reported by Phan and co-workers (Phan et al., 2013). 50 µL of the tested compounds in DMSO corresponding to a final concentration of 50 µg/mL in the net test solution was added to test tubes. To each test tube, 100 µL of α-amylase (5U/mL of porcine pancreatic α-amylase in 0.05 sodium phosphate buffer pH 6.8) and 460 µL of 0.05 M sodium phosphate buffer pH 6.8 were added. Like the α-glucosidase test, both 'Blank' and 'Positive Control' were also prepared. For both, 50 µL of DMSO was added instead of inhibitor and for 'Blank', 100 µL of buffer was added instead of the enzyme solution. Acarbose was also used as a standard in this test. The test tubes were left to shake at 37 ºC for 10 minutes. After which, 450 µL of 0.5% starch solution was added to each tube and all the tubes were left to shake at 37 ºC for another 20 minutes. Finally, 500 µL of dinitro salicylic acid (DNSA) reagent was added and the tubes were placed in a boiling water bath for 15 minutes. The absorbance of the tubes was then recorded at 540 nm and the percentage inhibition is calculated based on the same formula as shown in the case of α-glucosidase above. All measurements were performed in triplicates and the values are represented as mean ± standard deviation.

The 1M, pH 6.8 sodium phosphate stock solution was obtained by mixing 46.3 mL of 1M Na_2HPO_4 and 53.8 mL of 1M NaH_2PO_4. 1M pH 7.0 sodium phosphate stock solution was prepared by mixing 57.7 mL of 1M Na_2HPO_4 and 42.3 mL of 1M NaH_2PO_4. Subsequently, the stock solutions were diluted with deionized water to 0.05 M and 0.1 M for the respective tests. 0.5% starch solution was prepared by dissolving 0.5 g of starch in 99.5 mL of buffer. The starch solution

was heated in a boiling water bath for 5 minutes to ensure starch dissolved completely. DNSA reagent is prepared by mixing 1 g of dinitrosalicylic acid (DNSA) in 50.0 mL of deionized water. After which, 30.0 g of sodium tartrate was added slowly followed by 20.0 mL of 2N NaOH solution (8.00 g in 100 mL of water). Finally, the volume was topped up to 100 mL.

Results and Discussion

Chemistry

The route to synthesize 3,3-di(indoloyl)indolin-2-ones **1a**-**p** is shown in Scheme 1. The reaction between indoles **2** and isatins **3** in the presence of catalytic amount of BF_3 or H_2SO_4 at 40-60 ºC afforded the desired products **1a**-**1c**, **1f** and **1i**-**1p** in high 68-97% yields within 2 h. Compounds **1d, 1e** and **1g** were obtained conveniently in high 90-94% yields by alkylating their corresponding counterparts. The 3,3-di(indoloyl)indolin-2-ones **1a**-**p** were characterized using MS, IR, ^{1}H NMR and ^{13}C NMR and the spectral data were consistent with the structures and are typical for oxindole systems (Wang et al., 2017).

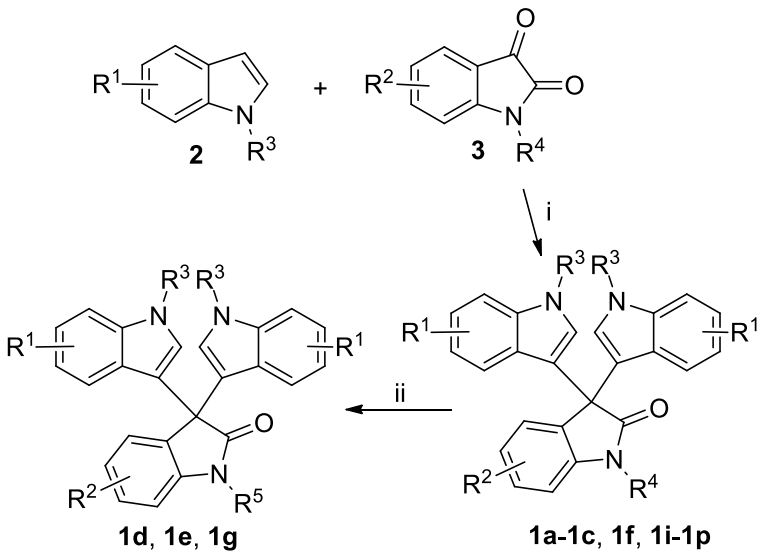

Reagents and conditions: (i) BF_3 or H_2SO_4, MeOH, 2 h, 40-60 ^oC; (ii) MeI, or EtI or Me_2SO_4, KOH, DMSO, 2 h, 0 ^oC to r.t

Scheme 1. Synthesis of 3,3-di(indolyl)indolin-2-ones **1a**-**p**

α-Glucosidase and α-Amylase Inhibition Studies

The α-glucosidase and α-amylase % inhibition activities of the synthesized 3,3-di(indoloyl)indolin-2-ones **1a**-**p** along with that of acarbose as the positive standard drug are summarized in Table 1. In general, while the compounds showed high to excellent inhibition activities for both enzymes, they showed stronger α-glucosidase inhibitory activity and desired lower α-amylase inhibitory activity in comparison to standard AGI drug acarbose.

α-Glucosidase Inhibition Activities

All the compounds showed higher % α-glucosidase inhibition activities ranging from 37±11 to 94±3 in comparison to acarbose with % inhibition activity of 19±5, all measured at a concentration of 50 µg/ml. An exception are compounds **1a** and **1h** which showed % inhibition activities of 16±6 and 17±3, respectively (Table 1, entries 1 and 8). Considering the compounds in Table 1, the type of substituent and their position played a role in the inhibition activities to

different extents. Compound **1a** with no substituents showed the lowest % inhibition activity of 16±6. In the study conducted by Wang *et.al*. (Wang et al., 2017) the same compound **1a** showed the lowest IC_{50} value of 145.95±0.46 µM. Introduction of a methyl moiety at the indole rings as in **1b** lead to doubling of the % inhibition activity to 37±11 while the introduction of an ethyl moiety as in **1c** increases the activity to more than four folds to 73±6. Interestingly, while the introduction of methyl moiety to the oxindole ring increased the inhibition activity of **1d** to 86±7, the introduction of a corresponding ethyl moiety as in **1e** reduced the activity to 50±11. This unpredicted result underscores the effect of small structural changes on the inhibitory activity. Compound **1f** with bromine moiety enhanced the % inhibition activity of its parent **1a** by five-folds from 16±6 to 76±8. However, compound **1g** with the bromine at the same position but with another at the indole rings gave lower inhibition activity of 61±1 in comparison to its parent **1d** with inhibition activity of 86±7. Introduction of strong electron donating NH_2 group on the oxindole ring of **1a** to give **1h** did not significantly affect the % inhibition activity (17±3 *vs* 16±6, entry 8 *vs* entry 1, Table 1). However, the introduction of additional OH groups on the indole rings of **1h** and replacing its NH_2 group with NO_2 group to give **1i**, significantly increased the % inhibition activity from 17±3 to 67±13 (Table 1, entry 8 *vs* entry 9). Additionally, stronger electron withdrawing NO_2 groups of **1j** increased its activity to almost five-fold (79±5 *vs* 16±6, Table 1, entry 10 *vs* entry 1). At this stage, we predicted that the introduction of *N*-alkyl substituents to **1j** will increase its inhibition activities. However, while compound **1k** with methyl substituents showed moderate increase in the % inhibition activity to 86±6, compound **1l** with benzyl substituent decreased the % inhibition activity to 76±8 perhaps due to stearic effects which prevented better fitting with the enzyme active sites. A significant increase in the activity occurred by changing the strong electron withdrawing NO_2 group of **1l** to bromine as in **1m** which showed

% inhibition of 92±3, or related **1n** which showed % inhibition of 94±3. Replacement of bromine of **1f** with chlorine to get **1o** resulted in a small increase in the % inhibition activity (Table 1, entry 6 *vs* entry 15). Methylation of **1o** with to obtain **1p** did not increase the % inhibition activity.

Table 1. Percentage inhibition of α-glucosidase and α-amylase by 3,3-di(indoloyl)indolin-2-ones **1a**-**p** with acarbose as the reference standard

No	Indolin-2-one	R^1	R^2	R^3	R^4/R^5	% α-glucosidase inhibition[a]	% α-amylase inhibition[a]
1	**1a**	H	H	H	H	16±6	92±4
2	**1b**	H	H	CH_3	H	37±11	81±6
3	**1c**	H	H	CH_3CH_2	H	73±6	72±5
4	**1d**	H	H	CH_3	CH_3	86±7	77±8
5	**1e**	H	H	CH_3CH_2	CH_3CH_2	50±11	74±9
6	**1f**	H	Br	H	H	76±8	86±10
7	**1g**	Br	Br	CH_3	CH_3	61±1	79±4
8	**1h**	H	NH_2	H	H	17±3	79±9
9	**1i**	OH	NO_2	H	H	67±13	51±4
10	**1j**	H	NO_2	H	H	79±5	93±6
11	**1k**	H	NO_2	CH_3	H	86±6	91±5
12	**1l**	H	NO_2	H	Benzyl	76±8	86±0

13	**1m**	H	Br	H	Benzyl	92±3	80±3
14	**1n**	H	Br	H	4-Br-benzyl	94±3	73±5
15	**1o**	H	Cl	H	H	83±2	87±6
16	**1p**	H	Cl	CH_3	H	84±2	81±7
17	Acarbose[a]					19±5	90±2

[a] Inhibition was measured at a concentration of 50 µg/ml. Inhibition values are expressed as means ± SD; n=3.

α-Amylase Inhibition Activities

The tested compounds in Table 1 showed high to very high α-amylase % inhibition activities ranging from 72±5 to 92±4, except **1i** which showed % inhibition value of 51±4, all measured at a concentration of 50 µg/ml. Overall, the differences in activities between structurally related compounds are not as pronounced as in the α-glucosidase case. Interestingly, compound **1a** which showed the lowest α-glucosidase inhibitory activity exhibited one of the highest α-amylase % inhibition activity of 92±4. The inhibition activity varied with the size/number of the substituents. For example, as the size/number of the substituents increases in compounds **1a-e**, the corresponding inhibition values decreases (Table 1, entries 1-5). The same is also observed for compounds **1f** and **1g**. The situation becomes ambiguous when we consider the effects of electron withdrawing and donating substituents which gave no obvious trend. For example, the parent compound **1a** showed very high % inhibition activity similar to compounds **1j** with 93±6 and **1k** with 91±5 having strong electron withdrawing group NO_2 and donating methyl moieties. The inhibition values in Table 1 suggest that compounds **1a-h** and **1j-p** have similar mode of interactions with α-amylase enzymes and that mode is different in case of **1i**. As mentioned in the

introduction section, lower α-amylase inhibition is desired to overcome the gastrointestinal side-effects. Therefore, compound **1i** serves this purpose considering that it has the lowest α-amylase activity and high α-glucosidase activity.

Molecular Docking Studies

Docking simulations were performed to reveal the binding modes of 3,3-di(indoloyl)indolin-2-ones **1a**, **1i**, and **1n** with α-glucosidase and α-amylase enzymes. The structure of the human lysosomal α-glucosidase (Mor and Sindhu, 2020) and human pancreatic α-amylase (Tysoe et al., 2019) was directly downloaded from the protein data bank (PDBID: 5NN5 and 6OCN, respectively) and was optimized after removing the co-factors, water molecules, and heteroatoms. The structures of the ligands were directly drawn using MarvinSketch program (Miladiyah et al., 2018). The docking simulation was conducted using Autodock 4.2.6 software (Hussain et al., 2020). The docking center was set to be the center of protein and the docking pocket size was set to be large enough to cover the whole protein molecule. The docking results were visualized using Discovery studio (Dassault Systèmes, San Diego) (Mohapatra et al., 2021).

Docking simulations were performed on 3,3-di(indoloyl)indolin-2-ones **1a**, **1i,** and **1n** to predict the binding interaction of these compounds in the active site of both enzymes. These compounds were selected because they showed the highest contrasting α-glucosidase and α-amylase inhibition values (Table 1, entries 1, 9, and 14). In the docking simulation, all the 3,3-di(indoloyl)indolin-2-ones **1a**, **1i,** and **1n** recognized the binding pocket of both enzymes correctly. These indolin-2-ones formed stable key interactions with the active sites of both enzymes.

In the case of α-glucosidase, the binding affinities of the three indolin-2-ones is in the order **1a** (-7.45 kcal/mol) > **1i** (-7.84 kcal/mol) > **1n** (-8.26 kcal/mol) which is consistent with the experimental % inhibition trend values 16±6 < 67±13 < 94±3, respectively. The theoretical binding

modes of compounds **1a**, **1i,** and **1n** with α-glucosidase are shown in Figure 1. Indolin-2-one **1a** formed hydrophobic π-σ interaction with the Trp376. One of the indole rings formed π-π T-shaped interaction with Phe649 and Trp481 while the other indole rings formed π-alkyl with Leu650 and Ala284. Both of the indole rings also formed π-anion interaction with Asp616. From the docking analysis, hydrogen bonds were observed between NH of each indole rings with Met519 (bond length: 2.93 Å) and Asp282 (bond length: 1.88 Å). Indolin-2-one **1i** which has an NO_2 and OH groups formed new hydrogen bonds with Leu677 (bond length: 2.34 Å) and Asp404 (bond length: 2.76 Å), respectively, while maintaining the hydrogen bond between the NH of the other indole rings and Asp282 (bond length: 2.06 Å). Additionally, the NO_2 group not only formed a conventional hydrogen bond, but also a non-classical or carbon-hydrogen bond with the Ser676.The OH group formed π-lone pair interaction with Trp376. However, it was different from indolin-2-one **1n** which did not show the presence of any hydrogen bonds. The *p*-bromobenzyl group on the indolin-2-one ring in indolin-2-one **1n** formed hydrophobic π-π stacking and π-alkyl interactions with Phe649, His674, Trp613, and Trp516 residues. In addition, the benzene ring of *p*-bromobenzyl group formed a π-anion interaction with Asp518. Besides, both indolin-2-ones **1i** and **1n** maintained the hydrophobic interaction with Trp376, Leu650, and Ala284 residues.

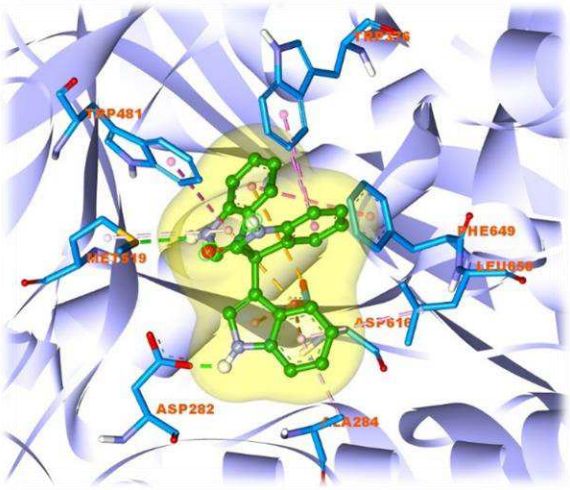

(a)

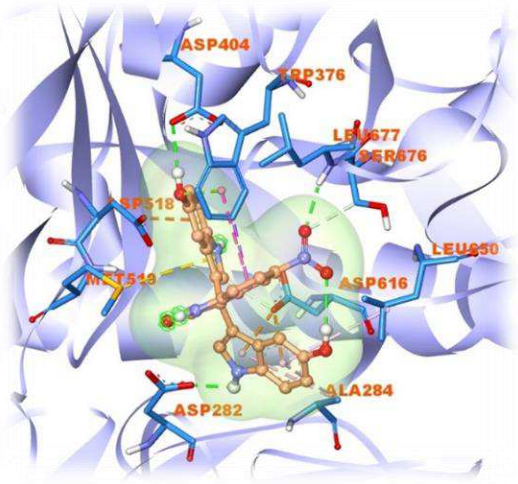

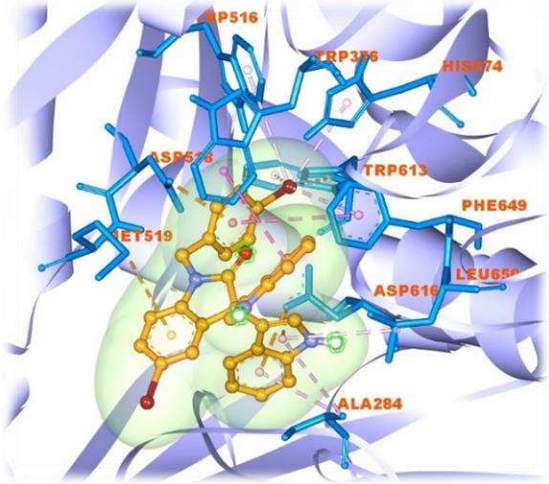

(b) (c)

Figure 1. Binding interaction of (a) indolin-2-one **1a**, (b) indolin-2-one **1i**, and (c) indolin-2-one **1n** in with α-glucosidase (PDB ID: 5NN5)

In the case of docking with α-amylase, the binding affinities of indolin-2-ones were in the order **1i** (-8.42 kcal/mol) > **1a** (-8.47 kcal/mol) > **1n** (-8.75 kcal/mol) which is different from the trend with α-glucosidase. The binding modes of indolin-2-ones **1a**, **1i,** and **1n** with α-amylase are shown in Figure 2. The protein-ligand complex analysis of compound **1a** showed there were two

kinds of hydrogen bonds observed on the indolin-2-one ring which were conventional and non-classical hydrogen bonds. The NH of the indolin-2-one ring formed the conventional hydrogen bond with Asp197 (bond length: 1.74 Å) while the carbonyl group of the indolin-2-one ring formed the non-classical hydrogen bond with His101 (bond length: 3.52 Å). The indole rings of compound **1a** formed several hydrophobic interactions which were π-σ interaction with Ile235 and Leu162, π-alkyl interaction with Ala198, Leu165, and Leu162. Moreover, there were electrostatic interactions via a π-cation interaction between the indolin-2-one ring and Glu233 then a π-anion interaction between one of the indole ring and His201. From the docking analysis, the carbonyl group of the indolin-2-one ring in compound **1i** formed non-classical hydrogen bond with His101 (bond length: 3.02 Å). One of the indole rings of compound **1i** formed π-alkyl, π-σ, and π-anion interactions with Ala198, Leu162, and His 201, respectively. The other indole rings formed π-π T-shaped and π-anion interactions with Tyr62 and GLu233, respectively. Meanwhile, the substitution of the OH group in the indole rings formed hydrogen bonds with Glu233 (bond length: 1.72 Å) and Asp300 (bond length: 1.83 Å). In this receptor, again, compound **1n** showed no hydrogen bond but had five types of hydrophobic interaction in its protein-ligand complex. The bromo group of the indolin-2-one ring formed an alkyl hydrophobic interaction with Leu165, while bromo group of the *p*-bromobenzyl of the indolin-2-one ring formed alkyl and π-alkyl interaction with Ile235 and His201, respectively. The *p*-bromobenzyl group also formed π-σ and π-cation interaction with Ile235 and His201, respectively. The indole rings of compound **1n** formed π-π stacking and π-π T-shaped interactions with Trp58 and Tyr62, respectively. Also, the indole rings formed π-anion interaction with Asp300 and Glu233.

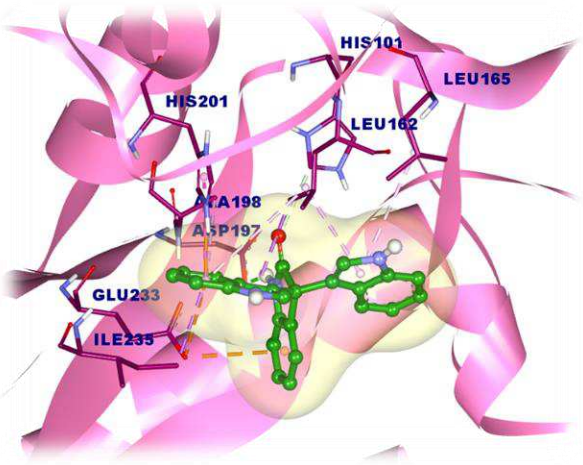

(a)

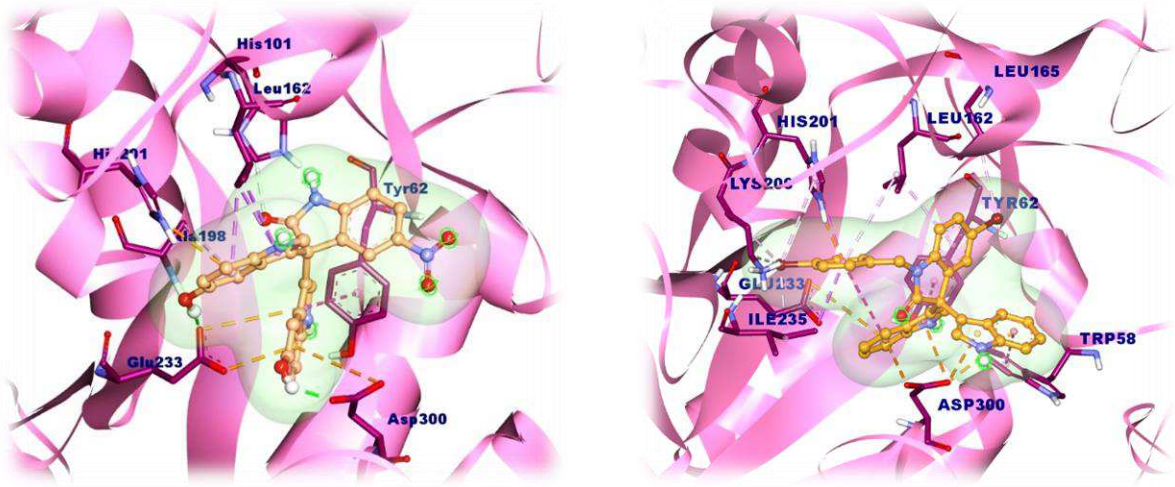

(b) (c)

Figure 2. Binding interaction of (a) indolin-2-one **1a**, (b) indolin-2-one **1i**, and (c) indolin-2-one **1n** with α-amylase (PDB ID: 6OCN)

Conclusions

We have synthesized a series of 3,3-di(indoloyl)indolin-2-ones **1a**-**p** and examined their α-glucosidase and α-amylase inhibitory activities. Overall, the compounds showed desired higher α-glucosidase activities and desired lower α-amylase activities than standard drug AGI acarbose.

The inhibitory activity against α-glucosidase varied greatly in comparison to α-amylase with respect to the substituents on the core structure. Molecular docking studies showed that the tested compounds interacted with the active sites of both α-glucosidase and α-amylase and the trend in the binding energy values parallel with the % inhibition values. The results suggest that 3,3-di(indoloyl)indolin-2-ones, especially indolin-2-one **1i**, are promising AGIs.

Acknowledgments

We would like to thank the Ministry of Science and Technology, Indonesia for funding M. Santoso and Z. Judeh through the World Class Professor Program. Financial help from Nanyang Technological University (RG142/16) is also acknowledged.

Conflict of interest

The authors confirm no conflict of interest.

References

Afifi AF, Kamel EM, Khalil AA, Foaad MA, Fawzi EM, Houseny M (2008) Purification and characterization of α-amylase from *Penicillium olsonii* under the effect of some antioxidant vitamins. Glob J Biotech Biochem 3: 14-21

Bergman J, Eklund N (1980) Synthesis and studies of tris-indolobenzenes and related compounds. Tetrahedron 36: 1445-1450

Blair M (2016) Diabetes mellitus review. Urol Nurs 36: 27-36

Brahmachari G, Banerjee B (2014) Facile and one-pot access of 3,3-bis(indol-3-yl)indolin-2-ones and 2,2-bis(indol-3-yl)acenaphthylen-1(2*H*)-one derivatives via an eco-friendly pseudo-

multicomponent reaction at room temperature using sulfamic acid as an organo-catalyst. ACS Sustain Chem Eng 2: 2802-2812

Chadha N, Silakari O (2017) Indoles as therapeutics of interest in medicinal chemistry: Bird's eye view. Eur J Med Chem 134: 159-184

DeFronzo RA, Ferrannini E, Groop L, Henry RR, Herman WH, Holst JJ, Hu FB, Kahn CR, Raz I, Shulman GI, Simonson GC, Testa MA, Weiss R (2015) Type 2 diabetes mellitus. Nat Rev Dis Primers 1: 15019

Derosa G, Maffioli P (2012) α-Glucosidase inhibitors and their use in clinical practice. Arch Med Sci 8: 899-906

El Sayed MT, Hamdy NA, Osman DA, Ahmed KM (2015) Indoles as anticancer agents. Adv Mod Oncol Res 1: 20-35

Gali R, Banothu J, Gondru R, Bavantula R, Velivela Y, Crooks PA (2015) One-pot multicomponent synthesis of indole incorporated thiazolylcoumarins and their antibacterial, anticancer and DNA cleavage studies. Bioorg Med Chem Lett 25: 106-112

Hussain MS, Azam F, Eldarrat HA, Alkskas I, Mayoof JA, Dammona JM, Ismail H, Ali M, Arif M, Haque A (2020) Anti-inflammatory, analgesic and molecular docking studies of lanostanoic acid 3-O-*α*-D-glycopyranoside isolated from *Helichrysum stoechas*. Arabian J Chem 13: 9196-9206

Kang WY, Song YL, Zhang L (2011) α-Glucosidase inhibitory and antioxidant properties and antidiabetic activity of *Hypericum ascyron*. Med Chem Res 20: 809-816

Karimi AR, Dalirnasab Z, Yousefi GH, Akbarizadeh AR (2015) Synthesis of mono and bis-[3,3-di(indolyl)indolin-2-ones] and evaluation of their antimicrobial activity. Res Chem Intermed 41: 10007-10016

Kelley DE, Bidot P, Freedman Z, Haag B, Podlecki D, Rendell M, Schimel D, Weiss S, Taylor T, Krol A, Magner J (1998) Efficacy and safety of acarbose in insulin-treated patients with type 2 diabetes. Diabetes Care 21: 2056–2061

Khan M, Yousaf M, Wadood A, Junaid M, Ashraf M, Alam U, Ali M, Arshad M, Hussain Z, Khan KM (2014) Discovery of novel oxindole derivatives as potent α-glucosidase inhibitors. Bioorg Med Chem 22: 3441-3448

Kim YM, Jeong YK, Wang MH, Lee WY, Rhee HI (2005) Inhibitory effect of pine extract on alpha-glucosidase activity and postprandial hyperglycemia. Nutrition 21: 756-761

Kothandapani J, Reddy SMK, Thamotharan S, Kumar SM, Byrappa K, Ganesan SS (2018) TBHP mediated substrate controlled oxidative dearomatization of indoles to C2/C3-quaternary indolinones. Eur J Org Chem 22: 2762-2767

Kwon YI, Apostolidis E, Shetty K (2007) Evaluation of pepper (*Capsicum annuum*) for management of diabetes and hypertension. J Food Biochem 31: 370-385

Miladiyah I, Jumina J, Haryana SM, Mustofa M (2018) Biological activity, quantitative structure–activity relationship analysis, and molecular docking of xanthone derivatives as anticancer drugs. Drug Des Dev Ther 12: 149-158

Mitra A, Dewanjee D, Dey B (2012) Mechanistic studies of lifestyle interventions in type 2 diabetes. World J Diabetes 3: 201-207

Mohapatra RK, Perekhoda L, Azam M, Suleiman M, Sarangi AK, Semenets A, Pintilie L, Al-Resayes SI (2021) Computational investigations of three main drugs and its comparison with synthesized compounds as potent inhibitors of SARS-CoV-2 main protease (M^{pro}): DFT, QSAR, molecular docking, and in silico toxicity analysis. J King Saud Univ Sci 33: 101315

Mor S, Sindhu S (2020) Synthesis, type II diabetes inhibitory activity, antimicrobial evaluation and docking studies of indeno[1,2-c]pyrazol-4(1H)-ones. Med Chem Res 29: 46–62

Paira P, Hazra A, Kumar S, Paira R, Sahu KB, Naskar S, Saha P, Mondal S, Maity A, Banerjee S, Mondal NB (2009) Efficient synthesis of 3,3-diheteroaromatic oxindole analogues and their in vitro evaluation for spermicidal potential. Bioorg Med Chem Lett 19: 4786-4789

Phan MAT, Wang J, Tang J, Lee YZ, Ng K (2013) Evaluation of α-glucosidase inhibition potential of some flavonoids from *Epimedium brevicornum*. LWT-Food Sci Technol 53: 492-498

Rad-Moghadam K, Sharifi-Kiasaraie M, Taheri-Amlashi H (2010) Synthesis of symmetrical and unsymmetrical 3,3-di(indolyl)indolin-2-ones under controlled catalysis of ionic liquids. Tetrahedron 66: 2316-2321

Reddy BVS, Rajeswari N, Sarangapani M, Prashanthi Y, Ganji RJ, Addlagatta A (2012) Iodine-catalyzed condensation of isatin with indoles: a facile synthesis of di(indolyl)indolin-2-ones and evaluation of their cytotoxicity. Bioorg Med Chem Lett 22: 2460-2463

Santos SA, Lukens AK, Coelho L, Nogueira F, Wirth DF, Mazitschek R, Moreira R, Paulo A (2015) Exploring the 3-piperidin-4-yl-1*H*-indole scaffold as a novel antimalarial chemotype. Eur J Med Chem 102: 320-333

Song YL, Wu F, Zhang CC, Liang GC, Zhou H, Yu JJ (2015) Ionic liquid catalyzed synthesis of 2-(indole-3-yl)-thiochroman-4-ones and their novel antifungal activities. Bioorg Med Chem Lett 25: 259-261

Srivastava SK, Agarwal A, Chauhan PMS, Agarwal SK, Bhaduri AP, Singh SN, Fatima N, Chatterjee RK (1999) Potent 1,3-disubstituted-9*H*-pyrido[3,4-*b*]indoles as new lead compounds in antifilarial chemotherapy. Bioorg Med Chem 7:1223–1236

Suresh B, Brahmeshwary G, Swamy T, Gopi I, Ravinder V (2016) Efficient synthesis of bis-indolyloxindoles from (phenylimino)indolin-2-ones and 1*H*-indole catalyzed by p-toluenesulfonic acid. Russ J Gen Chem 86: 1144-1150

Tysoe CR, Caner S, Calvert MB, Win-Mason A, Brayer GD, Withers SG (2019) Synthesis of montbretin A analogues yields potent competitive inhibitors of human pancreatic α-amylase. Chem Sci 10: 11073-11077

Wang G, Wang J, Xie Z, Chen M, Li L, Peng Y, Chen S, Li W, Deng B (2017) Discovery of 3,3-di(indolyl)indolin-2-one as a novel scaffold for α-glucosidase inhibitors: In silico studies and SAR predictions. Bioorg Chem 72: 228-233

Yoshikawa M, Murakami T, Yashiro K, Matsuda H (1998) Kotalanol, a potent alpha-glucosidase inhibitor with thiosugar sulfonium sulfate structure, from antidiabetic ayurvedic medicine *Salacia reticulate*. Chem Pharm Bull 46: 1339-1340

Zhang MZ, Chen Q, Yang GF (2015) A review on recent developments of indole-containing antiviral agents. Eur J Med Chem 89: 421-441

Figures

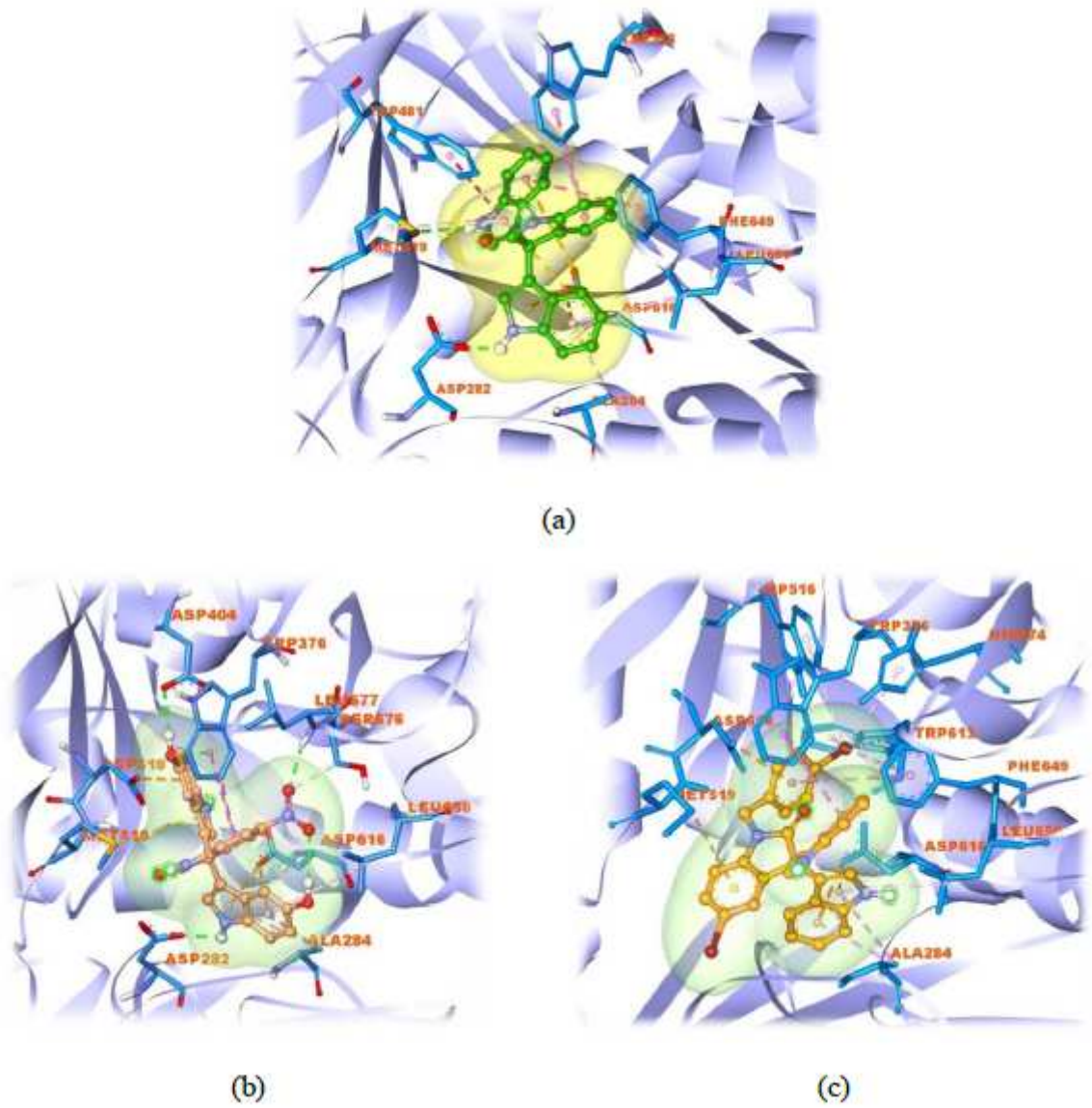

Figure 1

Binding interaction of (a) indolin-2-one 1a, (b) indolin-2-one 1i, and (c) indolin-2-one 1n in with α-glucosidase (PDB ID: 5NN5)

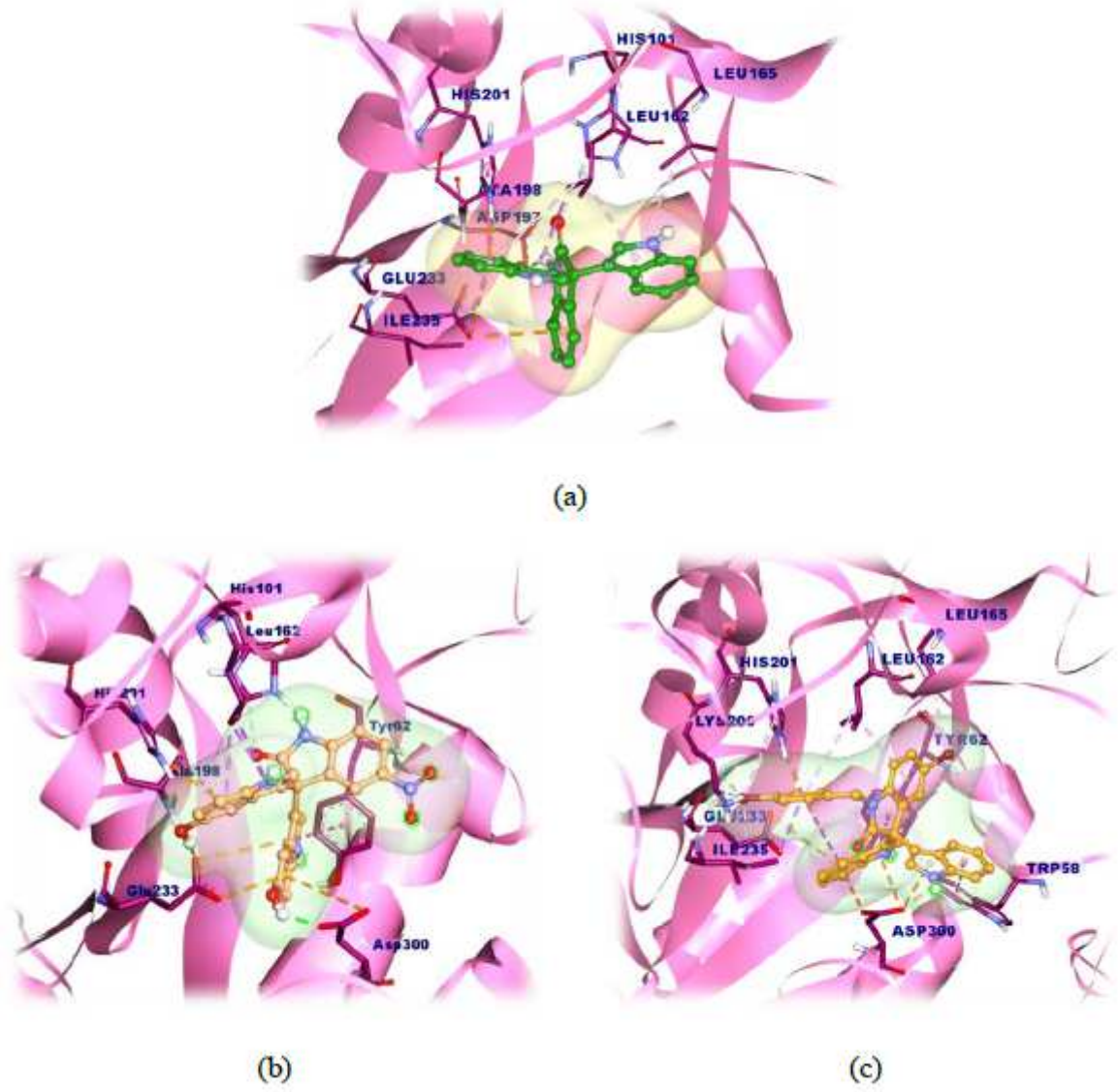

Figure 2

Binding interaction of (a) indolin-2-one 1a, (b) indolin-2-one 1i, and (c) indolin-2-one 1n with α-amylase (PDB ID: 6OCN)